

Evaluation of Arterial Signal Coordination with Commercial Connected Vehicle Data: Empirical Traffic Flow Visualizations and Performance Measures Considering Multiple Origin-Destination Paths

Shoaib Mahmud^a, Christopher M. Day^a

^a Department of Civil, Construction, and Environmental Engineering, Iowa State University, Ames, IA 50010, USA

ABSTRACT

Emerging connected vehicle (CV) data sets have recently become commercially available that enable analysts to develop a variety of powerful performance measures without a need to deploy field infrastructure. This paper presents a several tools using CV data to evaluate the quality of signal progression. These include both performance measures for high-level analysis as well as visualizations to examine details of coordinated operation. With the use of CV data, it is possible to assess not only the movement of traffic on the corridor but also to consider its origin-destination (O-D) path through the corridor, and the tools can be applied to select O-D paths or to all O-D paths in the corridor. Results for real-world operation of an eight-intersection signalized arterial are presented. A series of high-level performance measures are used to evaluate overall performance by time of day and direction, with differing results by metric. Next, the details of the operation are examined with the use of two visualization tools: a cyclic time space diagram, and an empirical platoon progression diagram. Comparing visualizations of only end-to-end journeys on the corridor with all journeys on the corridor reveals several features that are only visible with the latter. The study demonstrates the utility of CV trajectory data for obtaining high-level details as well as drilling down into the details.

keywords: *traffic signal timing, performance measures, vehicle trajectory data, connected vehicles*

INTRODUCTION

Traffic signal coordination facilitates the smooth, progressive flow of vehicle platoons along signalized corridors. Many arterial highways in the US are operated under actuated-coordinated control with time-of-day plans that implement timing plans to establish a flow pattern appropriate to expected demands during particular times of day, such as the morning and afternoon peak hours, off-peak periods, etc. Good progression reduces delay for travelers on the routes prioritized by coordination, which in many arterial highways is presumed to be the traffic which is served by the major street through movements at each intersection.

Floating car studies have historically been used to evaluate progression. The introduction of GPS instruments improved the data collection process, but still required that the analyst drive the floating cars to collect data. These types of studies are labor and equipment-intensive, involving substantial investments. More recently, advances in technology have enabled alternatives, such as measuring travel times using automated vehicle identification (1, 2), high-resolution traffic signal event data (2–6), and aggregated probe vehicle data (7–11). Automated traffic signal performance measures (ATSPMs) enabled by high-resolution data include visualizations such as the Purdue Coordination Diagram (PCD), which shows every detected vehicle arrival relative to individual green times. The presence of platoons and their arrival time relative to green intervals can be quickly ascertained from these views, distilled into aggregated metrics, and can also support optimization of offsets (6, 12, 13). However, attaining the supporting data requires that setback detectors and data collection equipment are available.

Use of vehicle trajectory data has also been used to develop performance measures on the operation of traffic signals and surface street networks (14–19). Previous studies that employed real-world data used data sources available internally to commercial data providers who, for various reasons, generally did not make such data available to others. That data was often obtained from onboard mobile devices, such as smartphones and navigation aids. In the past few years, multiple commercial providers have begun to market connected vehicle (CV) data aggregated from auto manufacturers and other original equipment manufacturer (OEM) sources. The utility of such data in evaluating traffic signal operations has been demonstrated in recent results from an ongoing pooled fund study (20).

The motivation for using commercialized CV data to assess operational performance is increasing in part because it requires no field data collection infrastructure, as noted in recent studies (20–24). Vehicle trajectory data makes it possible to obtain performance measures at any location along a signalized corridor without detection (25). The increasing availability of trajectory data from commercial CV sources enables a more accurate picture of corridor operations to be developed, which may permit consideration not only of the assumed dominant route along the corridor, but also for the performance of all origin-destination (O-D) paths through the corridor to be evaluated (26). As such data emerges, there is an opportunity to develop new tools for visualization and evaluation to support decision making.

The present paper demonstrates some uses of CV data for this purpose. The paper uses a signalized arterial corridor in Dubuque, Iowa, as a case study. O-D patterns through the network are assessed, performance measures are developed, and a series of visualizations are produced

that reveal signal operation using a cyclic view. The performance measures and visualizations can be prepared for selected O-D paths, or all observed CVs.

DATA SELECTION AND PROCESSING

Connected Vehicle Trajectory Data

Vehicle trajectories were obtained from a commercial vendor of CV data. The data consists of waypoint records including a journey ID, timestamp, vehicle position (latitude and longitude), speed as measured by the vehicle, heading, and other information. These records are able to track the movement of vehicles throughout the network, with a journey beginning when the vehicle ignition is turned on and ending when the vehicle is turned off. The waypoints are generally provided once every 3 seconds, although occasionally a waypoint would be missing.

Similar to other large datasets, use of CV data introduces challenges in data storage, processing, and sharing. In this study, a commercial cloud-based server (Amazon Athena) served as the main data repository, which supports SQL queries to perform tasks such as data processing and retrieval. The CV data were partitioned using zip codes, which permitted the selection of data relevant to the local area. Initial data cleaning and processing was performed on this server. The data were then exported in CSV format for further analysis for this study. Use of a cloud-based platform could permit scaling the analysis for on-demand analysis of any corridor in the statewide dataset, which is a subject for future research. However, use of such a server incurs additional cost. In addition to a strategy for managing a large dataset, potential automation requires a robust set of metadata to define corridors and intersections for purposes of analysis.

To extract data, a cordon was drawn around the corridor of interest, including the corridor itself and the approaches of the side streets. For the selected corridor (US 20 in Dubuque, Iowa), over 10.3 million GPS points in approximately 90,000 journeys were initially obtained within this corridor for 20 weekdays across 4 weeks in October 2021.

Next, journeys having a large number of missing waypoints (i.e., long intervals between waypoints) were removed. These mostly reflected vehicles on the edge of the cordon area whose traces were inadvertently captured in the previous geofencing process, but did not travel along the corridor. The data were later processed using R to remove journeys with fewer than five waypoints and waypoints more than 10 seconds apart. To limit the analysis to vehicles traveling between specific origins and destinations corresponding to the entry and exit points of the road, bounding boxes were drawn around these regions and only vehicles traversing at least two such regions were included. Some journeys were found traversing the corridor multiple times, making U-turns, or making temporary stops in roadside parking lots. These were excluded. After these processes, the data contained 53,656 unique vehicle journeys containing approximately 3.9 million waypoints over a four-week time period.

A map matching process was next undertaken to convert the latitude and longitude data used to store the positions into linear distance along the corridor to support visualization of trajectories and derivation of other performance measures. Road segment geometry was obtained from OpenStreetMap (27). Each waypoint was then “snapped” to a road segment using the closest

distance between the waypoint and the segment. This process was done in a “segment first” manner, meaning that we looked at each segment in turn and assigned waypoints to the segment, rather than trying to assign each waypoint to a particular segment. Incorrectly assigned waypoints could be easily removed since they would be either traveling in the opposite direction or, in the case of crossing streets, would have very few waypoints associated with the segment of interest. Whereas a more sophisticated map matching technique would be needed to scale the method to a wider analysis, this process was sufficient for the present study.

After map matching, it was possible to determine the penetration rate. It was found to be approximately 3–6%, assuming AADTs correspond to the corridor entering volume in both directions. The small penetration rate was mitigated by aggregation of data across multiple days of data, as demonstrated in previous studies for much lower penetration rates (25).

High-Resolution Data

ATSPMs based on high-resolution data have become a relatively common tool to evaluate signalized intersection performance (28). Although high-resolution data is not necessary for the CV-based methodology of this study, high-resolution data from the City of Dubuque was employed for two purposes: (1) to obtain the timing plan; and (2) to validate that the CV data can accurately capture traffic patterns by comparison with detector data. High-resolution data from the month of May, 2021 was used for this purpose.

High-resolution data includes records of timing plan changes. These were used to identify the timing plan as well as the cycle length. The weekday day plan on US 20 is as follows:

- Early morning, 06:30–08:00, Cycle Length = 109 sec
- Morning peak, 08:00–10:30, Cycle Length = 103 sec
- Midday, 10:30–14:30, Cycle Length = 115 sec
- Afternoon peak, 14:30–18:00, Cycle Length = 130 sec
- Evening, 18:00–22:00, Cycle Length = 103 sec

Signal systems running under time of day coordination often operate the same timing plan on all weekdays. US 20 in Dubuque runs under such a scheme. This makes it possible to aggregate multiple days of data to increase the number of samples, while still capturing patterns that are consistent from day to day, as demonstrated in previous work on probe data performance measures with small sample sizes of automatic vehicle identification data (29) and detector-free offset optimization (25). This paper adopts a similar strategy to increase the number of observations for preparation of performance measures. This strategy relies on the similarity of operation from day to day.

CORRIDOR ORIGIN-DESTINATION ANALYSIS

A 2.6-mile east-west section of US 20 in Dubuque, Iowa was selected for analysis. The corridor contains eight signalized intersections and is one of the busiest roads in that region. To understand the traffic patterns occurring on the corridor, an analysis of journeys by origin and destination was carried out. The data processing method described in the previous section resulted in every journey being associated with a particular origin and destination, making it

simple to perform this analysis. Origins and destinations for the test corridor are shown in Figure 1a, while Figure 1b shows an O-D matrix color coded to highlight the more dominant movements. For this part of the analysis, data from five weekdays in October 2021 was used.

We limited possible origins and destinations to roads entering or exiting the corridor and excluded driveways along the road. Those, however, could be easily added for a more detailed analysis, especially to better evaluate access management. The O-D matrix shows that although the largest volumes are for those paths traversing the corridor end-to-end (1E-8W and 8W-1E), Cedar Cross Rd (Int. 3) and NW Arterial (Int. 7) also attract and generate a substantial of traffic, with their numbers of originating or terminating journeys approximately 1/2 to 2/3 of that of the corridor endpoints.

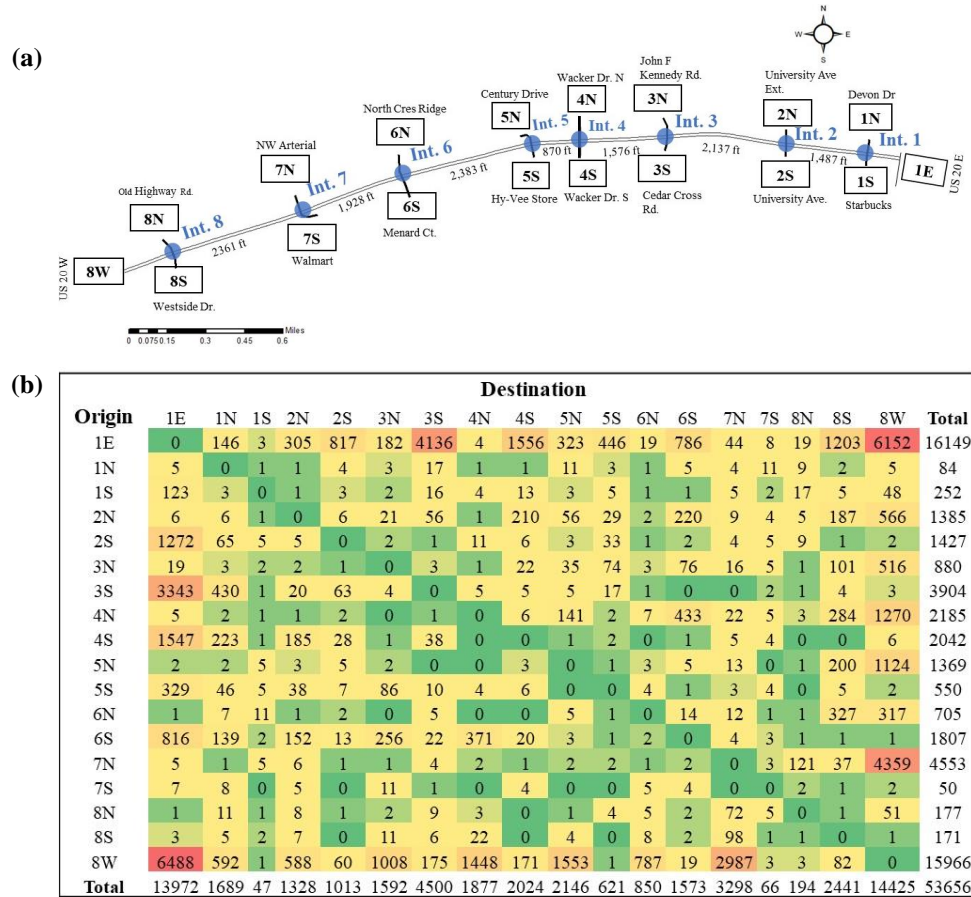


Figure 1. US-20 and trip count summary: (a) US-20 in Dubuque, IA with origins, destinations, and intersection IDs; (b) Journey count heatmap by origin-destinations with trajectory data

METHODOLOGY

Delay-Based Performance Measures

Travel time and delay are often used to evaluate corridor operations in floating car studies. Delay is used for intersection Level of Service (LOS) evaluations in the *Highway Capacity Manual*

(HCM). For evaluation of corridor performance, the HCM LOS uses the ratio of estimated travel time to free flow travel time (30). Such an analysis would typically only consider travel along the major through directions of the corridor, because it has traditionally been challenging to collect data for those paths alone. However, as the previous results have illustrated, there may be many different O-D paths on a corridor that are important to its operation. Recent studies have shown that consideration of O-D patterns can yield substantial improvements to signal timing (26).

A fundamental problem with comparing delay or travel time for different O-D paths is that each path has a different free flow travel time, depending on the distance and free flow speeds. One approach to resolving this is by normalizing the travel time, while another is to calculate delay. Two possible normalized metrics are the travel rate, and the travel time index (ratio of actual to ideal travel time).

The travel rate r_i experienced by vehicle i is defined as

$$r_i = \frac{t_i}{D} \quad \text{Equation 1}$$

where t_i is the observed travel time and D is the distance traveled.

The travel time index T_i is defined as

$$T_i = \frac{t_i}{t_f} \quad \text{Equation 2}$$

where t_i is the observed travel time, and t_f is the free flow travel time.

Delay d_i for vehicle i is defined as

$$d_i = t_i - t_f \quad \text{Equation 3}$$

where t_i is the observed travel time and t_f is the free flow travel time. In Equations 2 and 3, the speed limit may be used for t_f for simplicity, and to avoid potentially specifying an ideal travel time that may require exceeding the speed limit to achieve.

Smoothness of the Flow of the Traffic

The preceding metrics are concerned mainly with highly aggregate outcomes. Travel time and delay are single values that reveal the overall performance but reveal little about what occurs during the journey. As explored in a previous study, similar travel times can result from few stops or many stops, which may be reflected in addition of “stop penalties” to develop performance indices considering both travel time and stops (16). However, this necessitates

defining what a “stop” is, and it is a matter of opinion whether a vehicle that manages to avoid stopping by approaching an intersection slowly really fares that much better than a vehicle that pulls up and stops, at least from the viewpoint of the driver.

In anticipation of widespread trajectory data in future, Beak et al. (31) proposed a metric called the Smoothness of the Flow of Traffic (SOFT), which quantifies the platoon progression along a corridor using all of the speed changes encountered by the vehicle as it traverses the corridor. To calculate the metric, the authors calculated applied a fast Fourier transform of the frequency content of the speed data for each trajectory, yielding a score that tends to decrease as the trajectory shifts away from an ideal straight-line shape. SOFT is scaled from 0–100, with 100 representing ideal progression and lower values indicating poorer performance.

Beak defined SOFT for vehicle i as (32)

$$SOFT(i) = 100 \times \left(1 - \sqrt{\sum_{k=1}^{N-1} \left(\frac{P_k^i}{P_0^k} \right)^2} \right) \quad \text{Equation 4}$$

where $P_k^i = |X_k^i|^2$, which is given by the discrete Fourier transform (33):

$$X_k^i = \sum_{n=0}^1 s_i(nT_0) \exp \left[\frac{-2\pi k n j t}{T_0} \right] \quad \text{for } k = 0, 1, \dots, N-1 \quad \text{Equation 5}$$

In the above, $s_i(nT_0)$ is the speed of vehicle i at measurement nT_0 , where n is the measurement number and T_0 is the interval between measurements. Further information about the physical interpretation of SOFT is given by Beak (32). The resulting performance measure ranges from 0 to 100, with 100 representing an ideal trajectory shape, and lower values having an increasing amount of perturbations.

Figure 2 shows example calculations of SOFT for two trajectories, illustrated using a time-space diagram and a speed-time diagram. Figure 2a shows the trajectory of a vehicle that stops once, with a high SOFT value, while Figure 2b shows a vehicle that stops multiple times and has a much lower SOFT value.

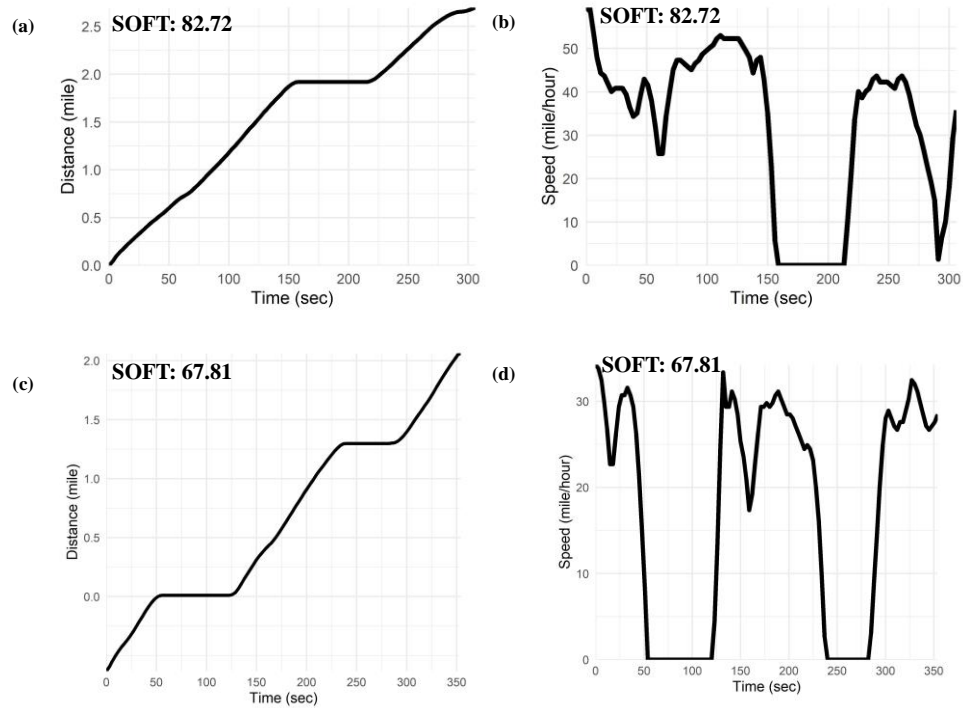


Figure 2. Trajectory and speed profile: (a) a vehicle experiencing few stops and slowdowns; (b) a vehicle that experiencing many stops and slowdowns.

The preceding metrics are calculated for each individual vehicle trajectory, which permits the development of distributions and aggregated values for additional assessment. For delay, we can simply take the total delay recorded by all vehicles on all the O-D paths to be included in the analysis:

$$X = \sum_{j \in Z} \left(\frac{1}{n_j} \sum_{i=1}^{n_j} d_i \right) \quad \text{Equation 6}$$

Here, n_j is the number of observations for OD path j , and the summation is carried out for all the O-D paths in set Z . Sets of O-D paths could be selected to include only routes in one direction, or only end-to-end movements, and other combinations desired by the analyst.

For the other performance measures, we take the weighted average:

$$X = \frac{\sum_{j \in Z} w_j \bar{x}_j}{\sum_{j \in Z} w_j} = \frac{\sum_{j \in Z} w_j \left(\frac{1}{n_j} \sum_{i=1}^{n_j} x_i \right)}{\sum_{j \in Z} w_j} \quad \text{Equation 7}$$

Here, X is the final aggregate performance measure, w_j is a weight value for O-D path j , \bar{x}_j is the average for O-D path j , n_j is the number of observations for O-D path j , and x_i is the i th observation.

The weight value used for each O-D path was the number of journeys observed on that path during the time period of interest. This could be adjusted if desired, for example to increase representation of certain paths with fewer observations.

Corridor Level Performance Visualization

In addition to quantitative performance measures, spatiotemporal visualizations are useful for transportation agencies to assess system-level operation and to discover the locations of problems and their nature. A time-space diagram (TSD) is one option and is particularly useful for viewing vehicle trajectories. Another visualization that may be particularly useful is the “platoon progression diagram,” (PPD) proposed in 1984 by Wallace and Courage (34). In this paper, we demonstrate the construction of a cyclic TSD and an empirical PPD.

The PPD is extremely similar to a cyclic flow profile, which was employed in the seminal work on flow-based optimization of traffic signal offsets (35) and in TRANSYT (36), which employed a mathematical platoon dispersion model for that purpose. The PPD is essentially an extension of the flow profile into a second spatial dimension. In its original form, platoon dispersion would be modeled up to a certain location on the downstream link, rather than all the way to the end of the link as in TRANSYT. The PPD is available as a visualization in more recent UK versions of TRANSYT and in the software Tru-Traffic. Since the PPD considers a spatial dimension, it could be considered a cyclic flow *and density* diagram.

The basis of both diagrams is a transformation of the time axis from a continuous to cyclic domain. The principle behind this can be derived from how most signal controllers determine their local clock time during coordination. For any given timestamp, the time of day t can be stated in terms of the number of seconds after a daily reference point. Most controllers use midnight as their default daily reference point. The time in cycle for an event occurring at t occurs at the following time in cycle (τ)

$$\tau = t \bmod C \quad \text{Equation 6}$$

where C is the cycle length (s) in effect at time t (s).

In graphical terms, the above transformation effectively truncates our TSD when the time axis reaches C , and causes the trajectories to “wrap around” to the other side. The distance axis does

not change. Whereas the resulting visualization no longer represents the condition of any particular cycle, the overlay of many trajectories in this view offers a useful way to assess locations where vehicles stop and slow down as they traverse the corridor. Furthermore, it is possible to select which O-D paths are included in the diagrams—for example, only those on the end-to-end trajectory, or all trajectories, including those that only partially traverse the corridor.

An empirical PPD can show similar data as cyclic distributions rather than overlaid trajectories, which represents the number of vehicles observed within any particular pixel, or a two-dimensional bin in a discretized time-space field. To create an empirical PPD, we begin by choosing time interval Δt and space interval Δx to divide up the relevant axes into discrete divisions. We used 1-second bins for Δt and 100 ft divisions for Δx . Using these divisions, it is possible to locate the address of any pixel in (x, t) coordinates where $t = [0, C - 1]$ and $x = [0, N_x]$, where N_x is the number of spatial divisions, given by

$$N_x = \text{floor} \left[\frac{L}{\Delta x} \right] \quad \text{Equation 7}$$

The “floor” function used above deletes the non-integer portion of the contained elements.

Figure 3 illustrates the construction of the basic elements of the cyclic TSD and the empirical PPD. Figure 3a shows two diagrams in which the transformation of Equation 6 has been applied to trajectory data. In the left side figure, the incorrect cycle length has been used, and the data are overlaid with no clear pattern. This is done purposefully to illustrate the effect of the slightest error in cycle length. The right side figure uses the correct cycle length, and cyclic flow patterns become apparent. It is clear that vehicles tend to stop at the first intersection, many of them stop at the second, and there are significant new vehicles entering the corridor after the second intersection, and so on. Figure 3b shows the further transformation of a few trajectories into the type of data representation for the PPD. Three trajectories are initially shown in a discretized time-space field. Next, for each pixel in that field, we count the number of trajectories that make an appearance within the relevant temporal and spatial divisions. We can then color-code these according to the pixel value to assist in the visualization.

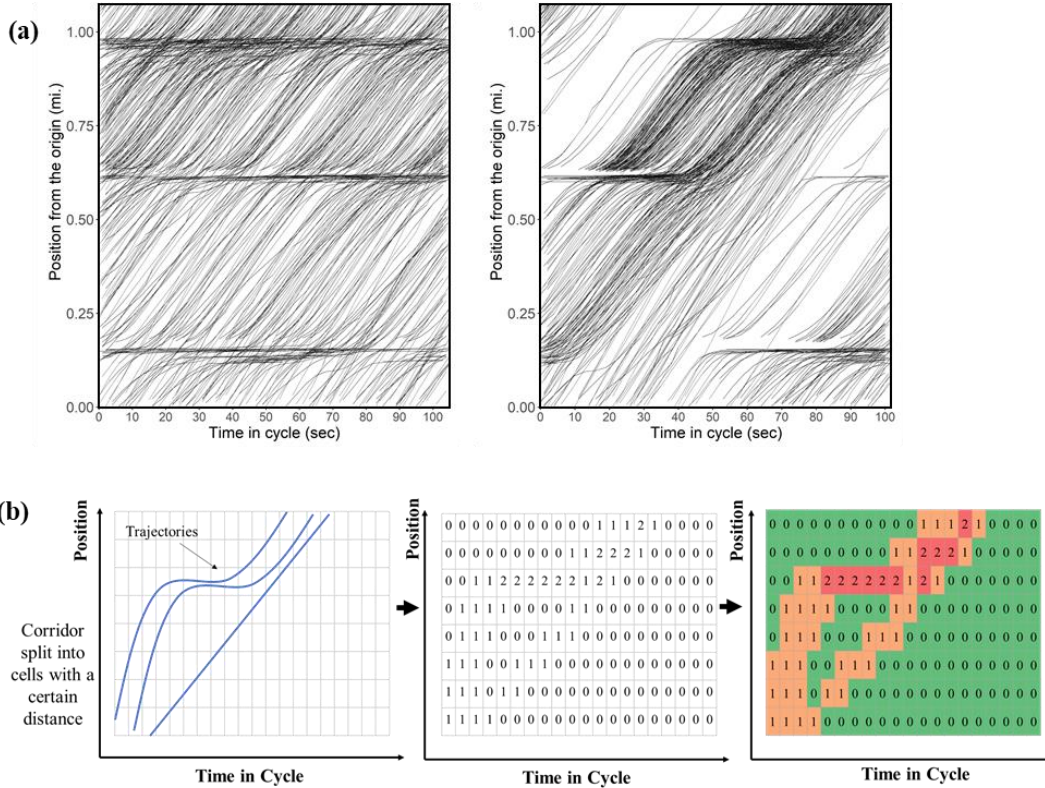


Figure 3. Development of empirical platoon progression diagram: (a) projection of trajectories into one representative cycle with incorrect cycle length vs correct cycle length (b) converting time space diagram to platoon progression diagram

CV data enables these visualizations to go further than previous iterations of the TSD and PPD, since the O-D path associated with each trajectory is known. Each of these visualizations can be done for any given O-D path in the network, as well as for selected O-D paths inside of that particular view. These visualizations permit the analyst to “drill down” from high-level aggregate values of the type described in the previous section, to examine details of the operation.

RESULTS

High-Level Performance Metrics for Different Timing Plans and O-D Paths

The weighted average method described in Equation 5 was used to combine the values of the quantitative performance measures presented earlier. This was done for each time of day plan. The outcomes of this process are illustrated by Figure 4. This figure also shows the total number of unique journey IDs per hour for each time-of-day period. For composite delay and average travel rate, larger values indicate worse performance, but the opposite is true for SOFT. Each diagram shows delay for the eastbound and westbound directions separately. Some selected observations are made below:

- For total delay, when considering all journeys (Figure 4a), westbound/afternoon peak exhibits the worst performance, followed by eastbound/midday. For end-to-end journeys (Figure 4b), the eastbound direction appears to do worse during both times of day. Also, comparing Figure 4b with Figure 4a shows that the total delay incurred by end-to-end journeys is much smaller than that of all journeys. The evening has the least delay, which is attributable to lower traffic volume during that time period. Unexpectedly, total delay for all journeys is higher for eastbound/early morning than in the same direction for the morning peak. This is likely because the travel demand in the eastbound early morning is similar to the morning peak (Figure 4g, Figure 4h), yet a different timing plan is in effect which may not serve the eastbound traffic as well as the morning peak timing plan.
- The average travel rate (Figure 4c and Figure 4d) shows rather similar results as delay for identifying the worst time periods. However, this metric is less affected by differences in volume from one time of day to another. The average travel time index had very similar results and is not included here. The average travel rate is slightly lower for end-to-end journeys, which is what would be expected since they are prioritized. Interestingly, the performance of the evening peak does not look as good using this metric. Although the total delay is lower because volumes are lower, the travel rate is comparable to other times of day.
- The average SOFT value is shown by Figure 4e and Figure 4f respectively for all journeys and end-to-end journeys. Lower values correspond to worse performance. These metrics show that eastbound/midday has the worst performance, followed by westbound/afternoon peak. The SOFT values experienced by end-to-end trips are higher, which again would be expected since this is the prioritized path. Drivers traversing the entire corridor also seem to fare worst on eastbound/midday, whereas in the afternoon peak the two directions are about the same. The evening peak has SOFT values that are only slightly better than the peak hours for end-to-end journeys.

In summary, the performance measures offer different perspectives on corridor performance, with different measures emphasizing aspects of performance. Use of multiple performance measures help reveal a more complete picture of what is occurring on the corridor. Total delay helps reveal the magnitude of cost to drivers, while average travel rate and SOFT are able to show the relative performance across time periods when volumes are different.

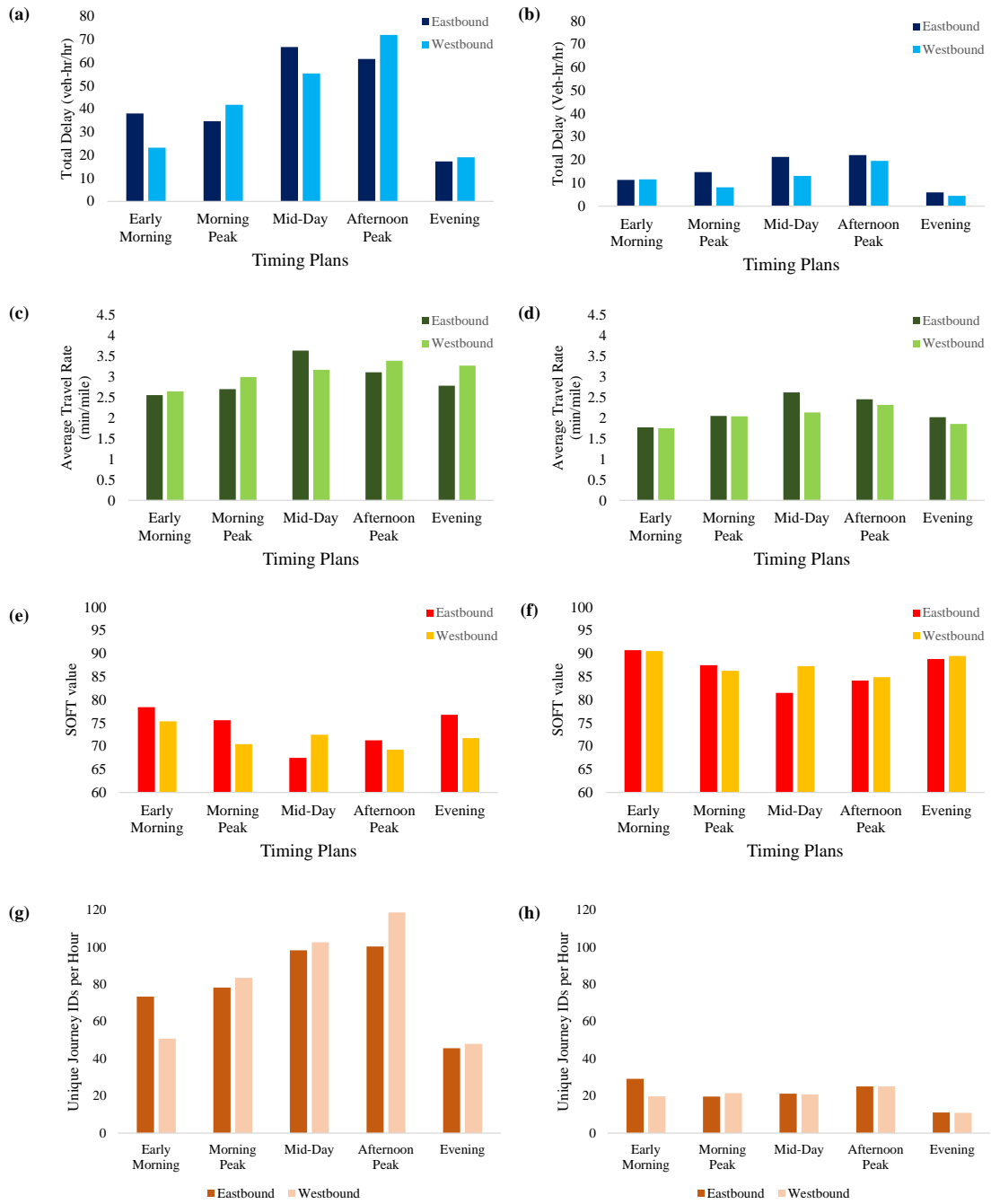


Figure 4. Comparison of the performance measure metrics: (a) composite delay for all routes; (b) composite delay for end-to-end journeys; (c) average travel rate for all routes; (d) average travel rate for end-to-end journeys; (e) average SOFT for all routes; (f) average SOFT for end-to-end journeys; (g) unique journey IDs per hour for all routes; (h) unique end-to-end journey IDs

Visualization of Corridor Performance

The aggregated performance measures offer a high-level view into the quality of progression. Visualizations of traffic flow can be used to better understand why a particular direction is performing well or poorly during a particular time of day. Using the processes described earlier, the vehicle trajectories were converted into cyclic TSDs and empirical PPDs. For illustrative purposes, two times of day are selected for a closer look: the morning peak, which tended to exhibit better performance in Figure 4, and the afternoon peak, which tended to exhibit worse performance.

Figure 5 shows cyclic TSDs for CVs traversing the entire corridor, which are easier to visualize at this scale than those containing all the journeys. In the latter case, the diagrams quickly become completely full of trajectory lines, and patterns are harder to identify. These figures are constructed to show two cycles next to each other to facilitate visualization. However, Cycle 2 is a repeat image of Cycle 1.

In Figure 4, for end-to-end journeys, during the afternoon peak, the westbound direction exhibited better performance than the eastbound direction, having lower total delay (Figure 4b), a lower travel rate (Figure 4d), and higher value of SOFT (Figure 4f), even though when all journeys were considered, the westbound direction ultimately had higher delay (Figure 4a) and lower SOFT (Figure 4e). Similarly, for the morning peak, the westbound direction tended to perform better than the eastbound direction when considering end-to-end journeys, but the opposite was true for all journeys.

These trends are also reflected in the cyclic TSDs (Figure 5). For the eastbound direction, in the morning peak (Figure 5a) the leading edge of the platoon is halted at N Cress Ridge (callout #1), Wacker Dr (#2), and experiences a long stop at Kennedy (#3), after which it is able to pass through the remaining intersections relatively easily (#4). In the afternoon peak (Figure 5b), there are more and longer stops and evidence of long queues. Evidence of queuing may be seen on the approach to NW Arterial (#5), Cress Ridge (#6), and the segment between Kennedy and Wacker nearly approaches spillback conditions (#7). The width of the platoon between Kennedy and University is very small (#8), illustrating that the green time in this direction is likely too short for the demand. The tail end of this platoon is cut off at University Ave (#9).

In contrast, the westbound direction performs relatively well in the morning peak (Figure 5c), although the end of the platoon is cut off at Kennedy (#10) and at Century (#11), and one rather long stop takes place at NW Arterial (#12). In the afternoon (Figure 5d), the platoon has a greater chance of being interrupted at certain points along the way, such as between University and Kennedy (#13), likely because of other traffic. Traffic is also stopped again at NW Arterial (#14). However, overall, the quality of progression is better than the other direction.

While these visualizations are useful, some of the trends are difficult to understand without being able to see other traffic besides the end-to-end journeys. It is sometimes also difficult to ascertain probably queue formation areas. Addition of the other journeys to the diagram might provide further insight, but as mentioned earlier, these inundate the diagrams with data and make it difficult to view individual trends. One option would be to select a smaller time period to

visualize, while another one is to employ the empirical PPD to show the same data in the form of cyclic distributions.

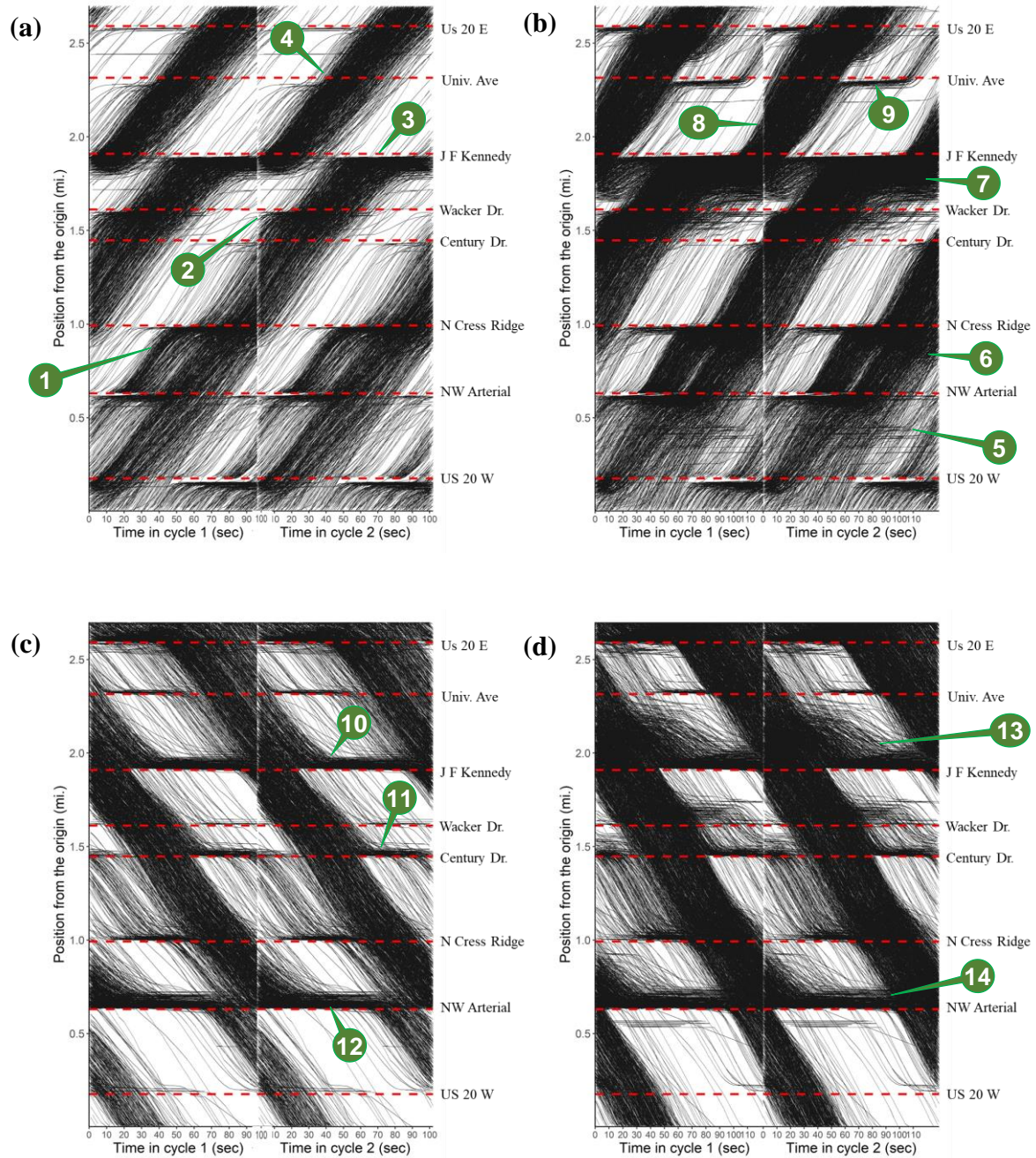


Figure 5. Cyclic TSDs for end-to-end vehicle trajectories: (a) eastbound/morning peak; (b) eastbound/afternoon peak, (c) westbound/morning peak; (d) westbound/afternoon peak

Figure 6 and Figure 7 show empirical PPDs for the morning peak and evening peak respectively. For each direction, two PPDs are prepared: one for all vehicles, and one for end-to-end vehicles only. Both diagrams use a color scale that shows the number of observations associated with each pixel. The more red, the greater the concentration of observations, meaning that there is higher flow over time in that area, and greater the density in that space during that time. Blue areas represent light traffic and white shows where no CVs were counted. The intermediate colors, mostly yellow, tend to show platoons. These diagrams illustrate the size, number, relative strength, and dispersion of platoons as they move through the corridor. Queuing is also evident, shown by greater concentrations of vehicles in regions close to an intersection, transforming from diagonal motion to horizontal stopping. These areas tend to exhibit the heaviest concentration of observations.

For the morning peak, the end-to-end journey PPDs (Figure 6a and Figure 6c) exhibit similar trends as seen in Figure 5, which is not surprising since they use the same data. Overall, the westbound direction (Figure 6c) appears to perform better than the eastbound direction (Figure 6a). The addition of the other traffic (Figure 6b and Figure 6d) presents a slightly different picture, however. When all journeys are included in the PPD, we can see that most of the westbound intersections exhibit some queueing (Figure 6d), and the performance starts to look rather similar to the eastbound direction (Figure 6b). The two PPDs do not appear to differ substantially from each other as much as when only end-to-end journeys were included. In addition, some new features appear that were not visible before. In the eastbound direction, a secondary platoons appears between Kennedy and University (callout #15), while in the westbound direction, several secondary platoons are evident on several segments, such as between University and Kennedy (#16), and on the next link (#17), and so on.

The end-to-end journey PPDs for the afternoon peak (Figure 7a and Figure 7c) again show similar trends as the cyclic TSDs. Addition of the other journeys (Figure 7b and Figure 7d) increases the amount of data considerably for this time of day, and the two directions of travel again show less difference from each other. Here as well we can see features emerge when all journeys are included in the PPD. Small secondary and tertiary platoons seem to be visible between Cress Ridge and Century (#18 and #19) in the eastbound direction. The link between Kennedy and University appears empty when looking only at end-to-end journeys (#20), but appears moderately busy when the other traffic is included (#21). In the westbound direction, a secondary platoon becomes visible between Century and Cress Ridge (#22), and the apparent empty space between NW Arterial and US 20 (#23) becomes full (#24).

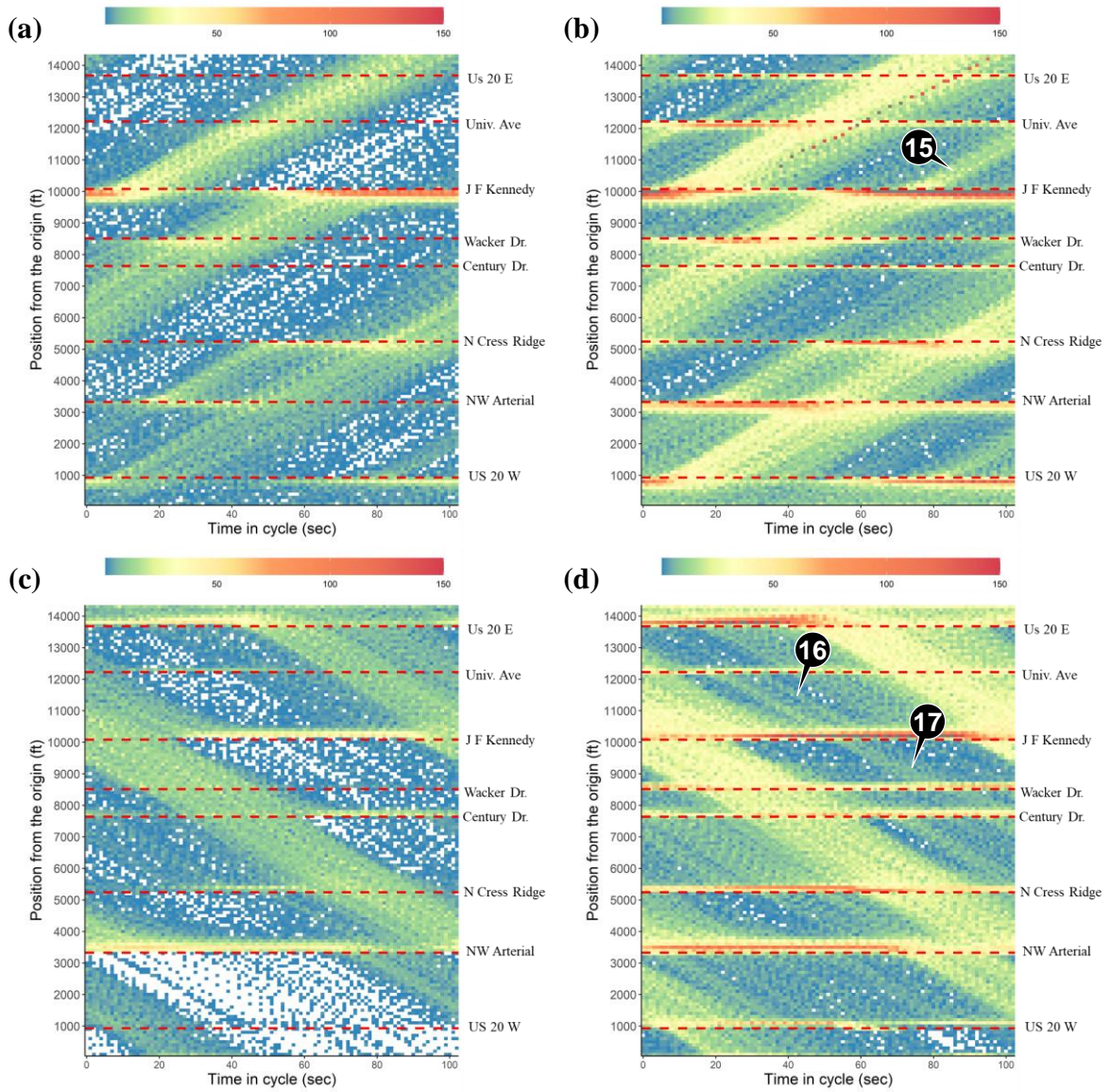


Figure 6. Empirical PPDs during the morning peak: (a) eastbound, end-to-end journeys; (b) eastbound, all journeys; (c) westbound, end-to-end journeys; (d) westbound, all journeys.

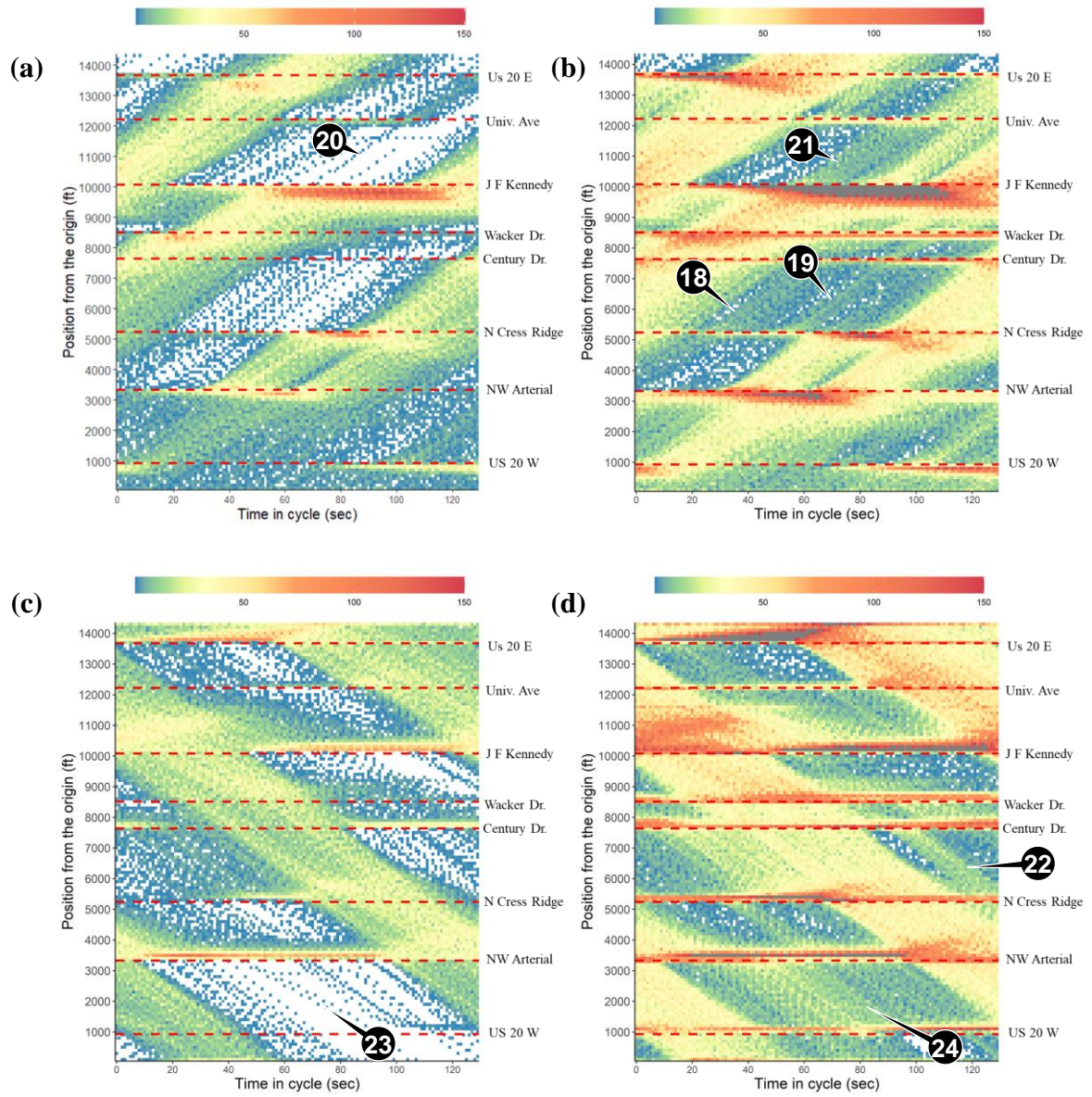


Figure 7. Empirical platoon progression diagrams during afternoon peak: (a) eastbound, end-to-end journeys; (b) eastbound, all journeys; (c) westbound, end-to-end journeys; (d) westbound, all journeys.

CONCLUSION

This paper presented a series of tools that employ connected vehicle (CV) data to evaluate and visualize the performance of signalized arterial corridors. The analysis was conducted using the case study of US 20 in Dubuque, Iowa, an 8-intersection corridor that experiences heavy traffic at certain times of day. CV data was obtained to support the analysis and initially validated with a comparison against high-resolution data. Next, the data were processed to convert the latitude/longitude positions into relative linear distance along road segments. Next, an O-D analysis was undertaken to identify the relative amounts of traffic flow on all possible paths between entry and exit points (excluding driveways, although they could be added in future).

A series of CV trajectory-based performance measures were then proposed for evaluating the quality of progression, including total delay, travel rate, travel time index, and SOFT. Of these, SOFT is the most recently proposed metric and is based on a Fourier transform of speed measurements to understand the degree to which the vehicle speeds are disturbed. Next, two visualizations were proposed to allow an analyst to see details of the performance: a cyclic time-space diagram (TSD) and an empirical platoon progression diagram (PPD).

Results were shown for US 20 using data from weekdays in October 2021. The high-level performance measures showed differing pictures depending on whether only end-to-end journeys were included, or all journeys. In some cases, one direction of travel would appear better than the other, for example. Visualizations using the TSD and PPD offered more detail. The TSDs revealed a great deal of information; however, these were prepared using only end-to-end journeys since inclusion of further journeys would start to hide the trends. The PPDs were able to show most of the same trends, but also supported addition of the other traffic, which revealed new features not visible before. Altogether, the visualizations offer a way to understand why certain times of day perform better or worse than others. In summary, the CV trajectory data offers both a means of evaluating high-level outcomes as well as low-level details.

Future research will expand upon this initial study to achieve several additional objectives. One of these is to develop an index for ranking multiple corridors (37). To accomplish this, additional performance measures should also be explored to investigate other aspects of the operation, such as queue length, the numbers of stops, prevalence of split failures, and so on. Future work will seek to extract data similar to that currently available from ATSPM systems. In addition, future work will attempt to infer signal timing from the CV trajectory data, introduce signal timing data into the TSD and PPD visualizations, and improve on previous methods of offset optimization by better considering the spatial dimension of the problem.

REFERENCES

1. Wasson, J. S. J. S., J. R. J. R. Sturdevant, and D. M. D. M. Bullock. Real-Time Travel Time Estimates Using Media Access Control Address Matching. *ITE Journal*, Vol. 78, No. 6, 2008, pp. 20–23.
2. Day, C. M., R. Haseman, H. Premachandra, T. M. Brennan, J. S. Wasson, J. R. Sturdevant, and D. M. Bullock. Evaluation of Arterial Signal Coordination: Methodologies for Visualizing High-Resolution Event Data and Measuring Travel Time. *Transportation Research Record*, No. 2192, 2010, pp. 37–49. <https://doi.org/10.3141/2192-04>.
3. Smaglik, E. J., D. M. Bullock, and A. Sharma. Pilot Study on Real-Time Calculation of Arrival Type for Assessment of Arterial Performance. *Journal of Transportation Engineering*, Vol. 133, 2007, pp. 415–422.
4. Day, C., D. Bullock, H. Li, S. Remias, A. Hainen, R. Freije, A. Stevens, J. Sturdevant, and T. Brennan. *Performance Measures for Traffic Signal Systems: An Outcome-Oriented Approach*. Purdue University, West Lafayette, Indiana, 2014.
5. Liu, H. X., and W. Ma. A Virtual Probe Vehicle Model for Time-Dependent Travel Time Estimation on Signalized Arterials. *Transportation Research Part C*, Vol. 17, 2009, pp. 11–26.
6. Hu, H., and H. X. Liu. Arterial Offset Optimization Using Archived High-Resolution Traffic Signal Data. *Transportation Research Part C: Emerging Technologies*, Vol. 37, 2013, pp. 131–144. <https://doi.org/10.1016/j.trc.2013.10.001>.
7. Mahmud, S., and C. M. Day. Leveraging Data-Driven Traffic Management in Smart Cities: Datasets for Highway Traffic Monitoring. In *The Rise of Smart Cities*, Elsevier, pp. 583–607.
8. Hainen, A. M., J. S. Wasson, S. M. L. Hubbard, S. M. Remias, G. D. Farnsworth, and D. M. Bullock. Estimating Route Choice and Travel Time Reliability with Field Observations of Bluetooth Probe Vehicles. *Transportation research record*, Vol. 2256, No. 1, 2011, pp. 43–50.
9. Remias, S. M., A. M. Hainen, C. M. Day, T. M. Brennan Jr, H. Li, E. Rivera-Hernandez, J. R. Sturdevant, S. E. Young, and D. M. Bullock. Performance Characterization of Arterial Traffic Flow with Probe Vehicle Data. *Transportation research record*, Vol. 2380, No. 1, 2013, pp. 10–21.
10. Hu, J., M. D. Fontaine, B. B. Park, and J. Ma. Field Evaluations of an Adaptive Traffic Signal—Using Private-Sector Probe Data. *Journal of Transportation Engineering*, Vol. 142, No. 1, 2016, p. 04015033. [https://doi.org/10.1061/\(ASCE\)TE.1943-5436.0000806](https://doi.org/10.1061/(ASCE)TE.1943-5436.0000806).
11. Hu, J., M. D. Fontaine, and J. Ma. Quality of Private Sector Travel-Time Data on Arterials. *Journal of Transportation Engineering*, Vol. 142, No. 4, 2016, p. 04016010. [https://doi.org/10.1061/\(ASCE\)TE.1943-5436.0000815](https://doi.org/10.1061/(ASCE)TE.1943-5436.0000815).
12. Day, C. M., and D. M. Bullock. Optimization of Traffic Signal Offsets with High Resolution Event Data. *Journal of Transportation Engineering, Part A: Systems*, Vol. 146, No. 3, 2020, p. 04019076. <https://doi.org/10.1061/JTEPBS.0000309>.
13. Day, C. M., and D. M. Bullock. Computational Efficiency of Alternative Algorithms for Arterial Offset Optimization. *Transportation Research Record*, No. 2259, 2011, pp. 37–47. <https://doi.org/10.3141/2259-04>.

14. Hofleitner, A., R. Herring, and A. Bayen. Arterial Travel Time Forecast with Streaming Data: A Hybrid Approach of Flow Modeling and Machine Learning. *Transportation Research Part B: Methodological*, Vol. 46, No. 9, 2012, pp. 1097–1122. <https://doi.org/10.1016/j.trb.2012.03.006>.
15. Wunsch, G., F. Bölling, A. von Dobschütz, and P. Mieth. Bavarian Road Administration's Use of Probe Data for Large-Scale Traffic Signal Evaluation Support. *Transportation Research Record: Journal of the Transportation Research Board*, Vol. 2487, No. 1, 2015, pp. 88–95. <https://doi.org/10.3141/2487-08>.
16. Day, C. M., and A. M. T. Emtenan. Trajectory-Based Performance Measures for Interrupted-Flow Facilities. *Strassenverkehrstechnik*, Vol. 63, 2019, pp. 647–653.
17. Argote, J., E. Christofa, Y. Xuan, and A. Skabardonis. Estimation of Measures of Effectiveness Based on Connected Vehicle Data. 2011.
18. Christofa, E., J. Argote, and A. Skabardonis. Arterial Queue Spillback Detection and Signal Control Based on Connected Vehicle Technology. *Transportation Research Record: Journal of the Transportation Research Board*, Vol. 2366, No. 1, 2013, pp. 61–70. <https://doi.org/10.3141/2356-08>.
19. Herrera, J. C., D. B. Work, R. Herring, X. (Jeff) Ban, Q. Jacobson, and A. M. Bayen. Evaluation of Traffic Data Obtained via GPS-Enabled Mobile Phones: The Mobile Century Field Experiment. *Transportation Research Part C: Emerging Technologies*, Vol. 18, No. 4, 2010, pp. 568–583. <https://doi.org/10.1016/j.trc.2009.10.006>.
20. Saldivar-Carranza, E., H. Li, J. Mathew, M. Hunter, J. Sturdevant, and D. M. Bullock. Deriving Operational Traffic Signal Performance Measures from Vehicle Trajectory Data. *Transportation Research Record: Journal of the Transportation Research Board*, Vol. 2675, No. 9, 2021, pp. 1250–1264. <https://doi.org/10.1177/03611981211006725>.
21. Mathew, J. K., J. C. Desai, R. S. Sakhare, W. Kim, H. Li, and D. M. Bullock. Big Data Applications for Managing Roadways. *ITE Journal*, Vol. 91, No. 2, 2021, pp. 28–35.
22. Claros, B., G. Vorhes, M. Chittur, A. Bill, and D. A. Noyce. Filling Traffic Count Gaps with Connected Vehicle Data. 2022.
23. Desai, J., E. Saldivar-Carranza, J. K. Mathew, H. Li, T. Platte, and D. Bullock. Methodology for Applying Connected Vehicle Data to Evaluate Impact of Interstate Construction Work Zone Diversions. 2021.
24. Saldivar-Carranza, E., H. Li, J. Mathew, C. Fisher, and D. M. Bullock. Signalized Corridor Timing Plan Change Assessment Using Connected Vehicle Data. *Journal of Transportation Technologies*, Vol. 12, No. 03, 2022, pp. 310–322. <https://doi.org/10.4236/jtts.2022.123019>.
25. Day, C. M., H. Li, L. Richardson, J. Howard, T. Platte, and D. M. Bullock. Detector-Free Optimization of Traffic Signal Offset with Connected Vehicle Data. *Transportation Research Record*, Vol. 2620, No. 54–68, 2017.
26. Xu, J., and Z. Tian. OD-Based Partition Technique to Improve Arterial Signal Coordination Using Connected Vehicle Data. *Transportation Research Record: Journal of the Transportation Research Board*, 2022, p. 036119812210986. <https://doi.org/10.1177/03611981221098692>.
27. OpenStreetMap Contributors. OpenStreetMap. <https://www.openstreetmap.org/>. Accessed Jul. 31, 2022.

28. Day, C. M., M. Taylor, J. Mackey, R. Clayton, S. K. Patel, G. Xie, H. Li, J. R. Sturdevant, and D. M. Bullock. Implementation of Automated Traffic Signal Performance Measures. *ITE Journal*, No. 8, 2016, pp. 26–34.
29. Young, S. E., E. Sharifi, C. M. Day, and D. M. Bullock. Visualizations of Travel Time Performance Based on Vehicle Re-Identification Data. *Transportation Research Record*, Vol. 2646, 2017, pp. 84–92.
30. *Highway Capacity Manual*. Publication Special Report 209. Transportation Research Board, Washington, DC, 2010.
31. Beak, B., K. L. Head, and S. Khoshmagham. Systematic Analysis of Traffic Signal Coordination Using Connected Vehicle Technology. 2017.
32. Beak, B. *Systematic Analysis and Integrated Optimization of Traffic Signal Control Systems in a Connected Vehicle Environment*. The University of Arizona, Tucson, Arizona, 2017.
33. Welch, P. The Use of Fast Fourier Transform for the Estimation of Power Spectra: A Method Based on Time Averaging over Short, Modified Periodograms. *IEEE Transactions on Audio and Electroacoustics*, Vol. 15, No. 2, 1967, pp. 70–73. <https://doi.org/10.1109/TAU.1967.1161901>.
34. Wallace, C. E., and K. G. Courage. Improved Graphic Techniques in Signal Progression. *Transportation Research Record*, Vol. 957, 1984, pp. 47–55.
35. Hillier, J. A., and R. Rothery. The Synchronization of Traffic Signals for Minimum Delay. *Transportation Science*, Vol. 1, 1967, pp. 81–94.
36. Robertson, D. I. *Transyt: A Traffic Network Study Tool*. Publication LR 253. Crowthorne, Berkshire, UK, 1969.
37. Day, C. M., S. M. Remias, H. Li, M. M. Mekker, M. L. McNamara, E. D. Cox, and D. M. Bullock. Performance Ranking of Arterial Corridors Using Travel Time and Travel Time Reliability Metrics. *Transportation Research Record*, Vol. 2487, No. 1, 2015, pp. 44–54. <https://doi.org/10.3141/2487-04>.